Correlation between parameters of pulse-type motions and damage of low-rise RC frames

Vui Van Cao[1], Hamid Reza Ronagh[2]
School of Civil Engineering, The University of Queensland, Australia

Abstract

The intensity of a ground motion can be measured by a number of parameters, some of which might exhibit robust correlations with the damage of structures subjected to that motion. In this study, 204 near-fault pulse-type records are selected and their seismic parameters are determined. Time history and damage analyses of a tested 3-storey reinforced concrete frame representing for low-rise reinforced concrete buildings subjected to those earthquake motions are performed after calibration and comparison with the available experimental results. The aim of this paper is to determine amongst several available seismic parameters, the ones that have strong correlations with the structural damage measured by a damage index and the maximum inter-story drift. The results show that *Velocity Spectrum Intensity* is the leading parameter demonstrating the best correlation, followed by *Housner Intensity*, *Spectral Acceleration* and *Spectral Displacement*. These seismic parameters are recommended as reliable parameters of near-fault pulse-type motions related to damage potential of low-rise reinforced concrete structures. The results also reaffirm that the conventional and widely used parameter of *Peak Ground Acceleration* does not exhibit a good correlation with the structural damage.

Keywords: Near-fault pulse-type motion; correlation; seismic parameter; damage index; reinforced concrete frame.

[1] PhD student. E-mail: v.caovan@uq.edu.au

[2] Corresponding author. Senior Lecturer, PhD. E-mail: h.ronagh@uq.edu.au

1 Introduction

The two Californian seismic events of the 1966 Parkfield and 1971 San Fernando possibly set the historical milestone of near-fault ground motions (Mavroeidis and Papageorgiou, 2003). The damage and failure of existing reinforced concrete (RC) structures in recent earthquakes (Northridge 1994, Kobe 1995, Chi-Chi 1999, Bam 2003, Christchurch 2011) have revealed their vulnerability. The extent of damage occurring in a structure caused by a ground motion primarily depends on two factors - the structure itself and the applied seismic loading. Deficiencies of structures have been confirmed as a major cause of the collapse of buildings during major recent earthquake events (Eleftheriadou and Karabinis, 2012; Ozmen et al., 2013; Yon et al., 2013). In the case of seismic loading, its intensity, energy and frequency contents play an important role in causing damage (Elnashai and Sarno, 2008; Moustafa and Takewaki, 2012). Near-fault ground motions greatly differ to those from far-fault (Choi et al., 2010; Kalkan and Kunnath, 2006); correspondingly, there has been a surge of studies on near-fault ground motion effects on structures (Kalkan and Kunnath, 2006). The special characteristics of near-fault earthquakes from the engineering point of view were first recognized by Bertero *et al* (1978). Generally, near-fault earthquakes are strong dynamic motions with high peak ground acceleration (PGA) (Lu and Lin, 2009), intense velocity (Galal and Naimi, 2008; Hatzigeorgiou, 2010; Lu and Lin, 2009), and large displacements (fling-step) (Galal and Ghobarah, 2006; Park et al., 2004). In addition, the characteristics of near-fault records are pulse-type (Baker, 2007) and long pulse-type period (2-5 s) (Galal and Naimi, 2008; Krishnan, 2007; Mollaioli et al., 2006).

There are many seismic parameters defined to represent the intensity of earthquake ground motions which seems to be at some degree related to the structural damage. The correlation between these seismic parameters and the damage of structures has been increasingly noticed by researchers (Alvanitopoulos et al., 2010). The inter-relationship between 10 seismic parameters of 20 well-known acceleration records and the maximum inter-storey drift, overall structural damage index and the maximum floor acceleration of a reinforced concrete building frame was investigated by Elenas (1997; 2000), Elenas and Liolios (1995), Elenas *et al* (1995; 1999), and Elenas and Meskouris (2001). They concluded that PGA exhibits a poor correlation while spectral and energy parameters well correlate with damage indices although they stated that further studies based on larger number of seismic records should be carried out in order to confirm the conclusions. Nanos *et al* (2008) examined the inter-relationship between the seismic parameters of strong motion durations of 450 artificial records and

overall damage indices of a 6-storey RC frame. They concluded that PGA and Arias intensity correlate with the damage indices well while the correlation between the parameters of strong motion durations and damage indices varied and depended on the definition of the duration.

The above-mentioned attempts addressed the issue of correlation between the seismic parameters and the damage of structures. However, none of them extensively addressed the correlation between the seismic parameters of near-fault pulse-type motions and the damage of structures. In this study, the three-storey RC frame tested by Bracci (1992) and published by Bracci *et al* (1995), is selected to represent low-rise reinforced concrete buildings and is modelled in SAP2000 (Computers and Structures Inc, 2009). The extent of information available in their reports makes it possible to have a thorough study of the structural behaviour numerically allowing direct and meaningful comparisons of the numerical results with experimental observations and data. After calibration, the analyses of the frame subjected to 204 selected near-fault pulse-type motions are performed. Next, damage analyses are conducted using the Park and Ang (1985) damage model and maximum inter-storey drift. Based on the findings of the correlation between the structural damage and the seismic parameters, conclusions are made as will be presented in the following.

2 Seismic parameters and selection of near-fault pulse-type motions

There are many seismic parameters available in the literature. They can be directly extracted from accelerograms and indirectly extracted using time history analysis (Elenas, 2000; Elenas and Meskouris, 2001). Those seismic parameters which are implemented in the software SeismoSignal ("SeismoSignal," 2010) are summarised the Table 1. The three spectral parameters of spectral acceleration, spectral velocity and spectral displacement are determined based on the corresponding response spectra given by the software SeismoSignal and the fundamental period of the structure. Hence, the total of 23 seismic parameters is used in this study. The definitions of those parameters were presented in the References in the Table 1 and can be viewed in the work by Kramer (1996) for a detailed description and discussion on the applications.

Table 1. Seismic parameters.

No.	Seismic parameter	Unit	Reference
1	Peak Ground Acceleration (PGA) (g)	g	
2	Peak Ground Velocity (PGV) (cm/s)	cm/s	
3	Peak Ground Displacement (PGD) (cm)	cm	
4	PGV / PGA	s	(Kramer, 1996)
5	Acceleration Root-mean-square (RMS)	g	(Dobry et al., 1978)
6	Velocity RMS	cm/s	(Kramer, 1996)
7	Displacement RMS	cm	(Kramer, 1996)
8	Arias Intensity	m/s	(Arias, 1970)
9	Characteristic Intensity	-	
10	Specific Energy Density	cm^2/s	
11	Cumulative Absolute Velocity (CAV)	cm/s	(EPRI, 1988)
12	Acceleration Spectrum Intensity (ASI)	g*s	(Housner, 1952; Thun et al., 1988)
13	Velocity Spectrum Intensity (VSI)	cm	(Housner, 1952; Thun et al., 1988)
14	Housner Intensity	cm	(Housner, 1952)
15	Sustained Maximum Acceleration (SMA)	g	(Nuttli, 1979)
16	Sustained Maximum Velocity (SMV)	cm/s	(Nuttli, 1979)
17	Effective Design Acceleration (EDA)	g	(Benjamin and Associates, 1988)
18	A95 parameter	g	(Sarma and Yang, 1987)
19	Predominant Period (Tp)	s	(Kramer, 1996)
20	Mean Period (Tm)	s	(Rathje et al., 1998)
21	Spectral acceleration	g	
22	Spectral velocity	cm/s	
23	Spectral displacement	cm	

Near-fault pulse-type motions used in this study are selected from the Pacific Earthquake Engineering Research Center database software (PEER, 2011). The selected 204 near-fault pulse-type records included in the software are shown in Table 2 with the names varying from 001 to 102 in the first column. The 23x204=4692 seismic parameters of 204 near-fault pulse-type records are then obtained using the software SeismoSignal ("SeismoSignal," 2010).

Table 2. Near-fault pulse type motions.

Name	NGA#	Event	Year	Station	Mag	Mechanism
001	150	Coyote Lake	1979	Gilroy Array #6	5.74	Strike-Slip
002	250	Mammoth Lakes-06	1980	Long Valley Dam (Upr L Abut)	5.94	Strike-Slip
003	316	Westmorland	1981	Parachute Test Site	5.9	Strike-Slip
004	319	Westmorland	1981	Westmorland Fire Sta	5.9	Strike-Slip
005	407	Coalinga-05	1983	Oil City	5.77	Reverse
006	415	Coalinga-05	1983	Transmitter Hill	5.77	Reverse
007	418	Coalinga-07	1983	Coalinga-14th & Elm (Old CHP)	5.21	Reverse
008	568	San Salvador	1986	Geotech Investig Center	5.8	Strike-Slip
009	569	San Salvador	1986	National Geografical Inst	5.8	Strike-Slip
010	615	Whittier Narrows-01	1987	Downey - Co Maint Bldg	5.99	Reverse-Oblique
011	645	Whittier Narrows-01	1987	LB - Orange Ave	5.99	Reverse-Oblique
012	158	Imperial Valley-06	1979	Aeropuerto Mexicali	6.53	Strike-Slip
013	159	Imperial Valley-06	1979	Agrarias	6.53	Strike-Slip
014	161	Imperial Valley-06	1979	Brawley Airport	6.53	Strike-Slip
015	170	Imperial Valley-06	1979	EC County Center FF	6.53	Strike-Slip
016	171	Imperial Valley-06	1979	EC Meloland Overpass FF	6.53	Strike-Slip
017	173	Imperial Valley-06	1979	El Centro Array #10	6.53	Strike-Slip
018	174	Imperial Valley-06	1979	El Centro Array #11	6.53	Strike-Slip
019	178	Imperial Valley-06	1979	El Centro Array #3	6.53	Strike-Slip
020	179	Imperial Valley-06	1979	El Centro Array #4	6.53	Strike-Slip
021	180	Imperial Valley-06	1979	El Centro Array #5	6.53	Strike-Slip
022	181	Imperial Valley-06	1979	El Centro Array #6	6.53	Strike-Slip
023	182	Imperial Valley-06	1979	El Centro Array #7	6.53	Strike-Slip
024	183	Imperial Valley-06	1979	El Centro Array #8	6.53	Strike-Slip
025	184	Imperial Valley-06	1979	El Centro Differential Array	6.53	Strike-Slip
026	185	Imperial Valley-06	1979	Holtville Post Office	6.53	Strike-Slip
027	451	Morgan Hill	1984	Coyote Lake Dam (SW Abut)	6.19	Strike-Slip
028	459	Morgan Hill	1984	Gilroy Array #6	6.19	Strike-Slip
029	529	N. Palm Springs	1986	North Palm Springs	6.06	Reverse-Oblique
030	721	Superstition Hills-02	1987	El Centro Imp. Co. Cent	6.54	Strike-Slip
031	722	Superstition Hills-02	1987	Kornbloom Road (temp)	6.54	Strike-Slip
032	723	Superstition Hills-02	1987	Parachute Test Site	6.54	Strike-Slip
033	2457	Chi-Chi, Taiwan-03	1999	CHY024	6.2	Reverse
034	2495	Chi-Chi, Taiwan-03	1999	CHY080	6.2	Reverse
035	2627	Chi-Chi, Taiwan-03	1999	TCU076	6.2	Reverse
036	3317	Chi-Chi, Taiwan-06	1999	CHY101	6.3	Reverse
037	3475	Chi-Chi, Taiwan-06	1999	TCU080	6.3	Reverse
038	77	San Fernando	1971	Pacoima Dam (upper left abut)	6.61	Reverse
039	292	Irpinia, Italy-01	1980	Sturno	6.9	Normal
040	496	Nahanni, Canada	1985	Site 2	6.76	Reverse
041	821	Erzican, Turkey	1992	Erzincan	6.69	Strike-Slip
042	983	Northridge-01	1994	Jensen Filter Plant Generator	6.69	Reverse
043	1009	Northridge-01	1994	LA - Wadsworth VA Hospital North	6.69	Reverse
044	1013	Northridge-01	1994	LA Dam	6.69	Reverse
045	1044	Northridge-01	1994	Newhall - Fire Sta	6.69	Reverse
046	1045	Northridge-01	1994	Newhall - W Pico Canyon Rd.	6.69	Reverse
047	1050	Northridge-01	1994	Pacoima Dam (downstr)	6.69	Reverse
048	1051	Northridge-01	1994	Pacoima Dam (upper left)	6.69	Reverse
049	1063	Northridge-01	1994	Rinaldi Receiving Sta	6.69	Reverse
050	1084	Northridge-01	1994	Sylmar - Converter Sta	6.69	Reverse
051	1085	Northridge-01	1994	Sylmar - Converter Sta East	6.69	Reverse
052	1086	Northridge-01	1994	Sylmar - Olive View Med FF	6.69	Reverse
053	1106	Kobe, Japan	1995	KJMA	6.9	Strike-Slip
054	1119	Kobe, Japan	1995	Takarazuka	6.9	Strike-Slip
055	1120	Kobe, Japan	1995	Takatori	6.9	Strike-Slip
056	738	Loma Prieta	1989	Alameda Naval Air Stn Hanger	6.93	Reverse-Oblique
057	763	Loma Prieta	1989	Gilroy - Gavilan Coll.	6.93	Reverse-Oblique
058	764	Loma Prieta	1989	Gilroy - Historic Bldg.	6.93	Reverse-Oblique

059	765	Loma Prieta	1989	Gilroy Array #1	6.93	Reverse-Oblique
060	766	Loma Prieta	1989	Gilroy Array #2	6.93	Reverse-Oblique
061	767	Loma Prieta	1989	Gilroy Array #3	6.93	Reverse-Oblique
062	779	Loma Prieta	1989	LGPC	6.93	Reverse-Oblique
063	784	Loma Prieta	1989	Oakland - Title & Trust	6.93	Reverse-Oblique
064	802	Loma Prieta	1989	Saratoga - Aloha Ave	6.93	Reverse-Oblique
065	803	Loma Prieta	1989	Saratoga - W Valley Coll.	6.93	Reverse-Oblique
066	825	Cape Mendocino	1992	Cape Mendocino	7.01	Reverse
067	828	Cape Mendocino	1992	Petrolia	7.01	Reverse
068	838	Landers	1992	Barstow	7.28	Strike-Slip
069	879	Landers	1992	Lucerne	7.28	Strike-Slip
070	900	Landers	1992	Yermo Fire Station	7.28	Strike-Slip
071	1602	Duzce, Turkey	1999	Bolu	7.14	Strike-Slip
072	1605	Duzce, Turkey	1999	Duzce	7.14	Strike-Slip
073	1148	Kocaeli, Turkey	1999	Arcelik	7.51	Strike-Slip
074	1176	Kocaeli, Turkey	1999	Yarimca	7.51	Strike-Slip
075	1182	Chi-Chi, Taiwan	1999	CHY006	7.62	Reverse-Oblique
076	1193	Chi-Chi, Taiwan	1999	CHY024	7.62	Reverse-Oblique
077	1202	Chi-Chi, Taiwan	1999	CHY035	7.62	Reverse-Oblique
078	1244	Chi-Chi, Taiwan	1999	CHY101	7.62	Reverse-Oblique
079	1410	Chi-Chi, Taiwan	1999	TAP003	7.62	Reverse-Oblique
080	1411	Chi-Chi, Taiwan	1999	TAP005	7.62	Reverse-Oblique
081	1463	Chi-Chi, Taiwan	1999	TCU003	7.62	Reverse-Oblique
082	1464	Chi-Chi, Taiwan	1999	TCU006	7.62	Reverse-Oblique
083	1468	Chi-Chi, Taiwan	1999	TCU010	7.62	Reverse-Oblique
084	1471	Chi-Chi, Taiwan	1999	TCU015	7.62	Reverse-Oblique
085	1473	Chi-Chi, Taiwan	1999	TCU018	7.62	Reverse-Oblique
086	1475	Chi-Chi, Taiwan	1999	TCU026	7.62	Reverse-Oblique
087	1476	Chi-Chi, Taiwan	1999	TCU029	7.62	Reverse-Oblique
088	1477	Chi-Chi, Taiwan	1999	TCU031	7.62	Reverse-Oblique
089	1479	Chi-Chi, Taiwan	1999	TCU034	7.62	Reverse-Oblique
090	1480	Chi-Chi, Taiwan	1999	TCU036	7.62	Reverse-Oblique
091	1481	Chi-Chi, Taiwan	1999	TCU038	7.62	Reverse-Oblique
092	1482	Chi-Chi, Taiwan	1999	TCU039	7.62	Reverse-Oblique
093	1483	Chi-Chi, Taiwan	1999	TCU040	7.62	Reverse-Oblique
094	1484	Chi-Chi, Taiwan	1999	TCU042	7.62	Reverse-Oblique
095	1486	Chi-Chi, Taiwan	1999	TCU046	7.62	Reverse-Oblique
096	1489	Chi-Chi, Taiwan	1999	TCU049	7.62	Reverse-Oblique
097	1492	Chi-Chi, Taiwan	1999	TCU052	7.62	Reverse-Oblique
98	1493	Chi-Chi, Taiwan	1999	TCU053	7.62	Reverse-Oblique
99	1494	Chi-Chi, Taiwan	1999	TCU054	7.62	Reverse-Oblique
100	1496	Chi-Chi, Taiwan	1999	TCU056	7.62	Reverse-Oblique
101	1498	Chi-Chi, Taiwan	1999	TCU059	7.62	Reverse-Oblique
102	1499	Chi-Chi, Taiwan	1999	TCU060	7.62	Reverse-Oblique

3 Damage indices

Various concepts and models for damage index are currently available in the literature. Some damage models based on changing stiffness or the flexibility of a structure were proposed by Roufaiel and Meyer (1981) and Banon et al (1981), which was later modified by Roufaiel and Meyer (1987). DiPasquale et al (1990) proposed an index based on the changing fundamental period called “final softening”, which was later exploited by Kim et al (2005). Ghobarah et al (1999) adopted a technique similar to DiPasquale et al (1990) and Kim et al (2005) but

replaced the fundamental period terms by the stiffness parameters of the structure to assess the extent of damage.

Plastic deformation, which closely relates to the damage states of structures, was also employed to invent damage models. The ratio of maximum plastic deformation and plastic deformation capacity was proposed as a damage index by Powell and Allahabadi (1988). The idea was further developed by Mergos and Kappos (2009) who recently proposed a concept for damage index that combined the flexural damage (D_{fl}) and shear damage (D_{sh}) of a structure to incorporate the shear deformations.

The damage suffered by a structure in an earthquake depends not only on the response magnitude but also the number of load cycles (Colombo and Negro, 2005). Hence, cumulative damage models are more rational to evaluate the damage states of structures, especially for those experiencing cyclic loading or earthquake excitation. In a simple way, Banon and Veneziano (1982) used normalised cumulative rotation as a damage index. They had it expressed by the ratio of the sum of inelastic rotations during half cycles to the yield rotation.

The amount of energy absorbed by a structure is closely related to its corresponding damage state. Hence damage index may be expressed as the ratio of the hysteretic energy demand (E_h) to the absorbed energy capacity of a structure under monotonic loading ($E_{h,u}$) (Fajfar, 1992; Rodriguez and Padilla, 2009). Park and Ang (1985) proposed a damage index based on deformation and hysteretic energy due to an earthquake as shown in Equation 1, where, u_m is the maximum displacement of a single-degree-of-freedom (SDOF) system subjected to earthquake, u_u is the ultimate displacement under monotonic loading, E_h is the hysteretic energy dissipated by the SDOF system, F_y is the yield force and β is a parameter to include the effect of cyclic loading. Park and Ang (1985) also proposed the damage indices for the individual storey and for the overall structure using the weighting factor based on hysteretic energy.

$$DI = \frac{u_m}{u_u} + \beta \frac{E_h}{F_y u_u} \tag{1}$$

This is well-known and the most widely used damage index (Kim et al., 2005), largely due to its general applicability and the clear definition of different damage states. Park and Ang's (1985) concept has been widely adopted and modified by researchers such as Fardis et al (1993), Ghobarah and Aly (1998) and Bozorgnia and Bertero (2001). However, the most

significant modification was made by Kunnath et al (1992). Despite the modifications made, the original Park and Ang model is still widely used. Examples of recent use are Yüksel and Sürmeli (2010), Bassam *et al* (2011), and Ghosh *et al* (2011). The drawbacks of the Park and Ang index - larger than 0 in elastic range and no specific upper limit (Cao et al., 2014) - would be helpful for correlation analysis; thus, this damage index was used in the current study.

Five levels of damage were classified by Park and Ang (1985) as shown in Table 3. The legends in the first column of Table 3 are added to describe the corresponding damage levels in the frame presented in Section 4. DI $\geq$ 0.8 to represent collapse suggested by Tabeshpour et al (2004) is adopted in this study.

Table 3. Damage levels.

Legend	Damage index	Description
.	DI < 0.1	No damage or localized minor cracking
+	0.1 $\leq$ DI < 0.25	Minor damage: light cracking throughout
x	0.25 $\leq$ DI < 0.40	Moderate damage: severe cracking, localized spalling
▲	0.4 $\leq$ DI < 1 (0.8)	Severe damage: concrete crushing, reinforcement exposed
●	DI $\geq$ 1 (0.8)	Collapse

4 Description and analysis of a tested three-storey frame

Figure 1 shows a one-third scaled three-storey reinforced concrete frame designed only for gravity load (Bracci, 1992). Its dimensions (in inches) and reinforcing details are presented in Figure 2. Concrete strength varied from 20.2 to 34.2 MPa (the average can be taken as f_c' = 27.2 MPa), and the average modulus of elasticity was taken as $E_c = 24200$ MPa. Four types of reinforcement were used, and their properties are shown in Table 4.

Table 4. Properties of reinforcement.

Reinforcement	Diameter (mm)	Yield strength (MPa)	Ultimate strength (MPa)	Modulus (MPa)	Ultimate strain
D4	5.715	468.86	503.34	214089.8	0.15
D5	6.401	262.01	372.33	214089.8	0.15
12 ga.	2.770	399.91	441.28	206160.5	0.13
11 ga.	3.048	386.12	482.65	205471	0.13

The dead loads were calculated from the self-weight of beams, columns, slabs and additional weights attached to the model, as shown in Figure 1. The total weight of each floor was found to be approximately 120 kN. Further details of the frame can be found in the references (Bracci, 1992) and (Bracci et al., 1995). The seismic record selected for simulation was the

N21E ground acceleration component of Taft earthquake occurred on 21 July 1952 at the Lincoln School Tunnel site in California. The PGAs are 0.05g, 0.20g and 0.30g representing minor, moderate and severe shaking, respectively. The axial loads in columns are assumed to be constant during excitations and are shown in Table 5.

Figure 1. The three storey frame (Bracci et al., 1995).

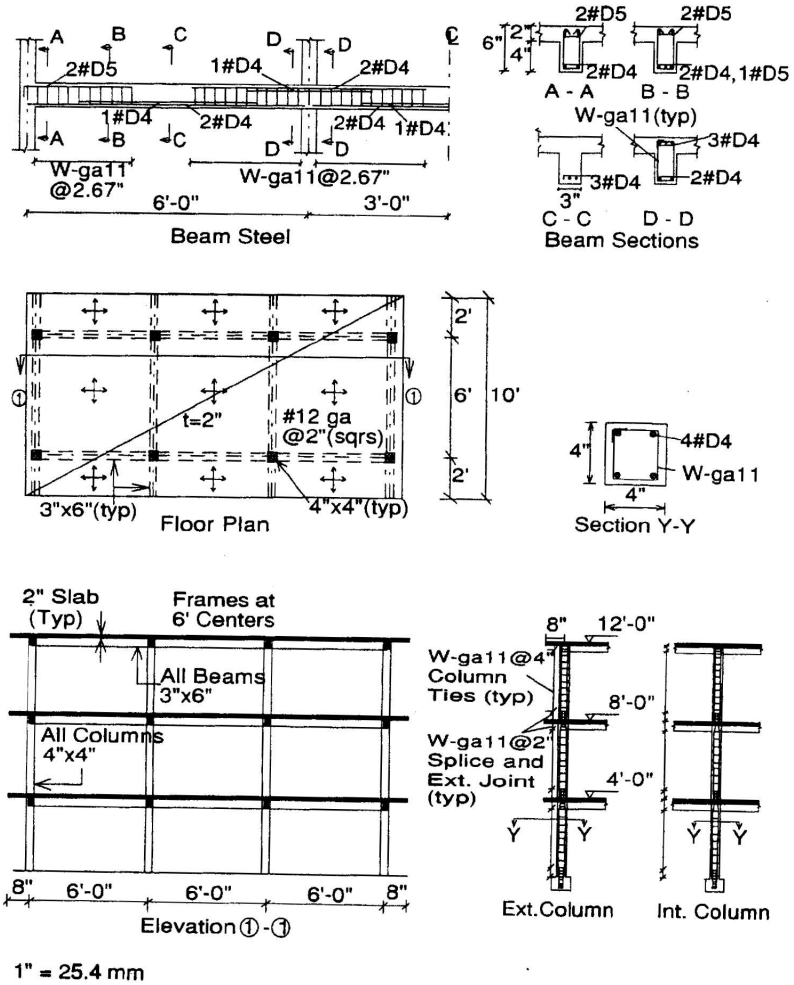

Figure 2. Dimensions and reinforcement arrangement of the three storey frame model (Bracci et al., 1995).

Table 5. Axial load in columns.

Storey	Axial load (kN)	
	External column	Internal column
1	30	60
2	20	40
3	10	20

The frame is modelled using the plastic hinge technique. The plastic hinge length $l_p = h$ proposed by Sheikh and Khoury (1993) and based on the observation from the experiment of the frame was adopted, in which, h is the depth of beams or columns. The plastic hinges are modelled using nonlinear Link elements. The behaviour of these nonlinear Link elements follows the hysteretic Takeda model (Takeda et al., 1970), which is selected to use in this paper because of its detailed descriptions and incorporation of the crack of concrete in the tension zone. The properties of nonlinear Link elements are computed based on the plastic hinge length l_p and moment-curvature curves. The moment-curvature curves are obtained using fibre model. The modification factors of 0.35 and 0.7 for EI_g of beam and column elements, respectively, recommended by ACI (2008) are adopted. Figure 3 shows the locations of Nonlinear Link elements, in which, h_{beam} and h_{column} is the depth of beams and columns, respectively, and Figure 4 shows model of the frame in SAP2000 (Computers and Structures Inc, 2009). The first three mode shapes are shown in Figure 5, and their structural frequencies are provided in Table 6 in comparison with the experimental results. They are very close in the first and second modes, but slightly different in the third mode. However, the first mode plays the most important role.

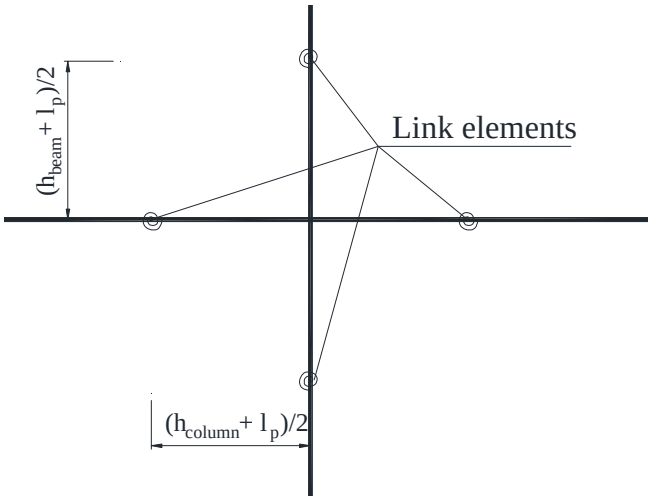

Figure 3. Locations of nonlinear Link elements.

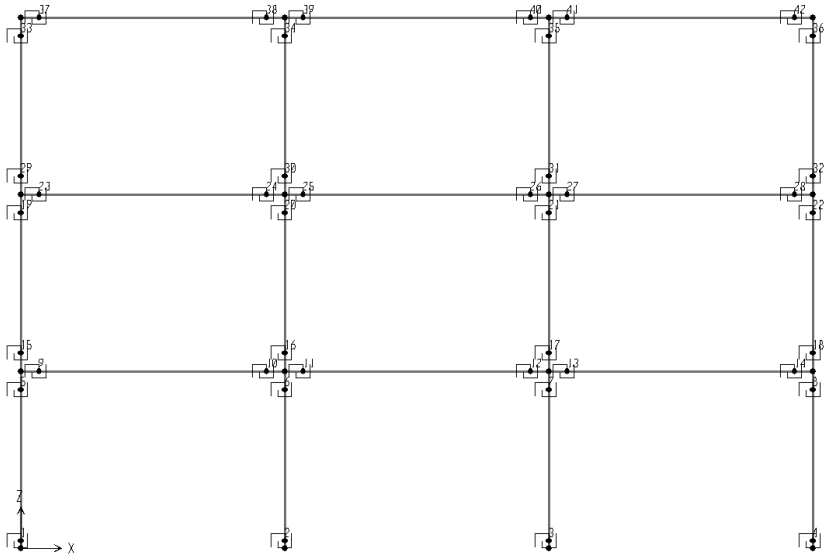

Figure 4. Modelling of the three-storey frame with Link elements.

a)

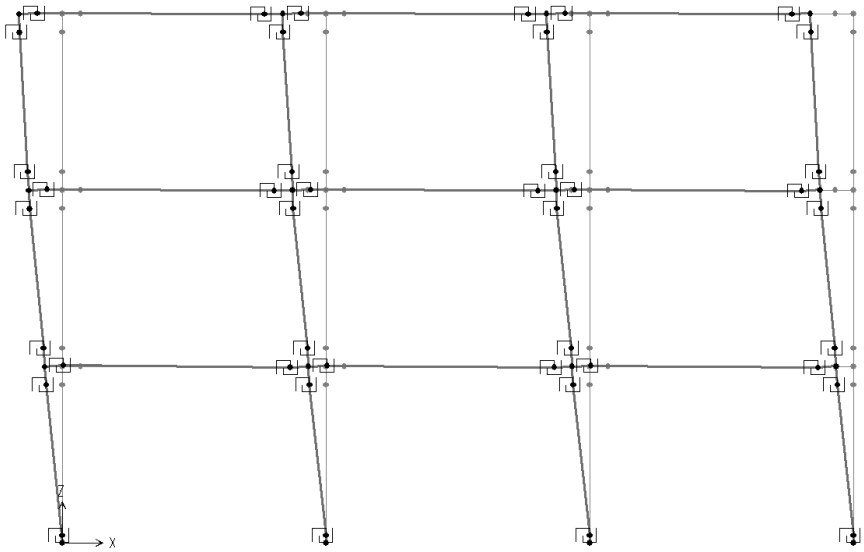

b)

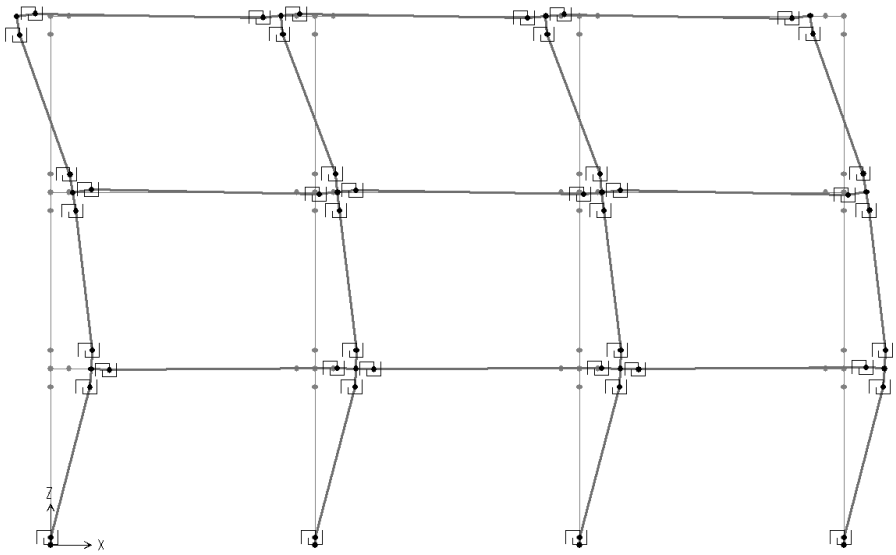

c)

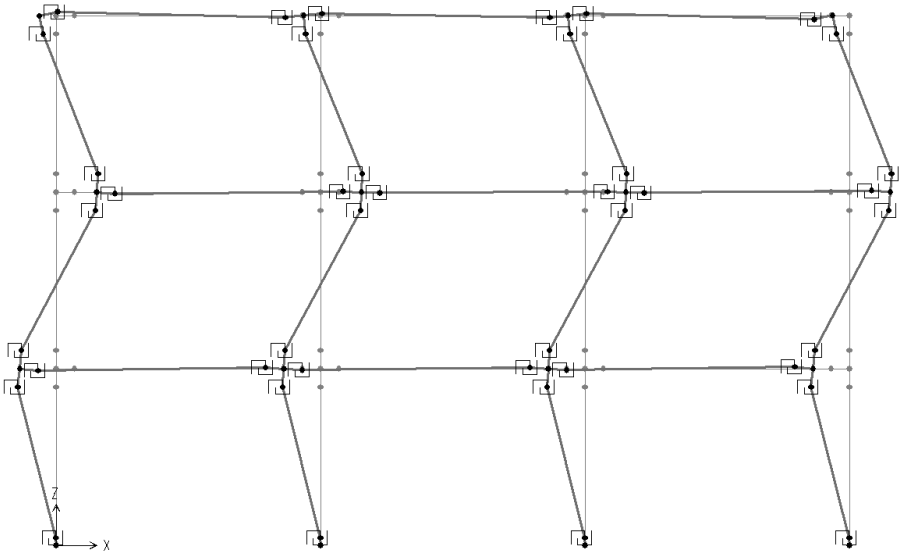

Figure 5. Mode shapes: a) Mode 1; b) Mode 2; b) Mode 3.

Table 6. Modal frequencies (Hz).

Mode	Experiment (Bracci et al., 1995)	Model
1	1.78	1.70
2	5.32	5.30
3	7.89	9.03

Table 7 presents a comparison between experimental (Bracci et al., 1995) and analytical results in terms of maximum inter-storey drift and maximum storey displacement. Though not an exact match, the model provides an overall good approximation.

Table 7. Comparison between experimental (Bracci et al., 1995) and analytical results.

PGA	Storey	Maximum inter-storey drift (%)		Maximum storey displacement (mm)	
		Experiment	Model	Experiment	Model
0.05g	3	0.23	0.21	7.6	7.9
	2	0.24	0.25	5.6	5.6
	1	0.28	0.23	3.6	2.8
0.20g	3	0.54	0.83	33.5	38.9
	2	1.07	1.17	29.0	30.7
	1	1.33	1.31	16.3	16.0
0.3g	3	0.89	1.18	59.7	58.4
	2	2.24	1.91	52.1	46.1
	1	2.03	1.96	24.6	23.9

After time history analyses, the damage occurred in the frame during the excitations is quantified by the selected Park and Ang (1985) damage model. The analytical damage states presented in Figures 6b, 7b and 8b are compared with the experimental damage states (Bracci, 1992) shown in Figures 6a, 7a and 8a for the Taft PGAs of 0.05g, 0.20g and 0.30g,

respectively. It is worth noting that different damage levels plotted in Figures 6b, 7b and 8b are referred to the legends expressed in Table 3. The analytical damage states of the frame clearly distinguish for the three shaking levels and are overall close to those obtained from experiment. It is worth noting that, in the analytical damage states, DI < 0.1 corresponding to "localized minor cracking" or "no damage" occurs in most of the locations in the frame.

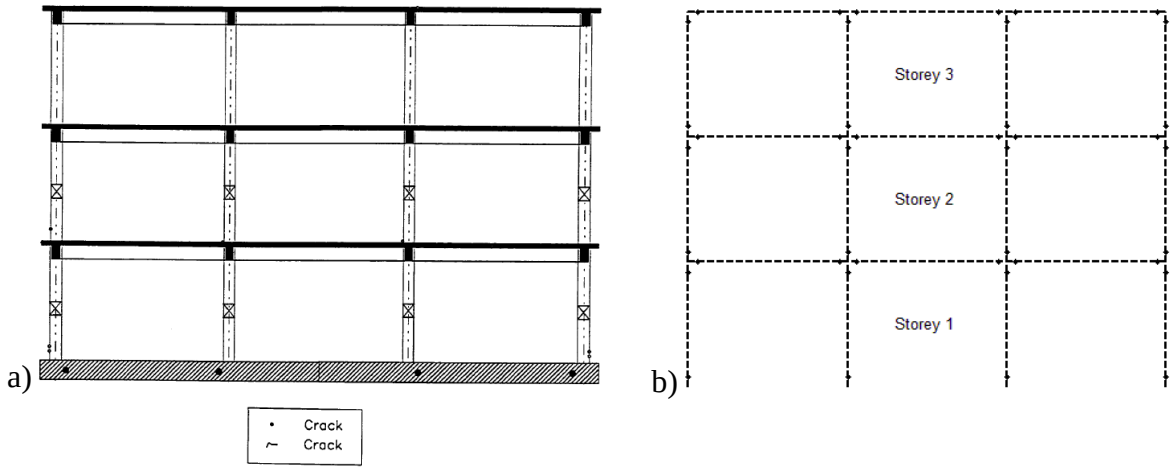

Figure 6. Damage state – Taft 0.05g: a) Experiment (Bracci, 1992); b) Analysis.

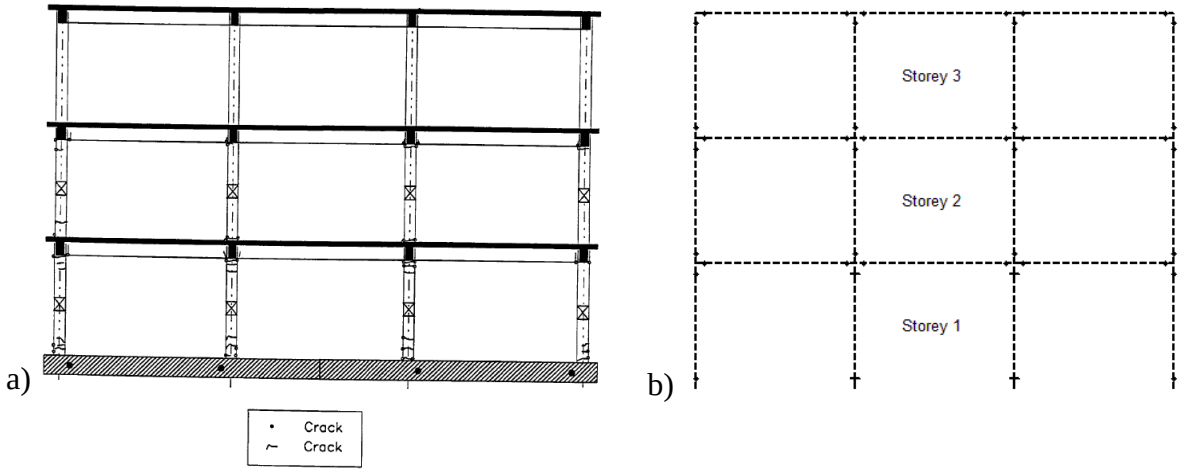

Figure 7. Damage state – Taft 0.20g: a) Experiment (Bracci, 1992); b) Analysis.

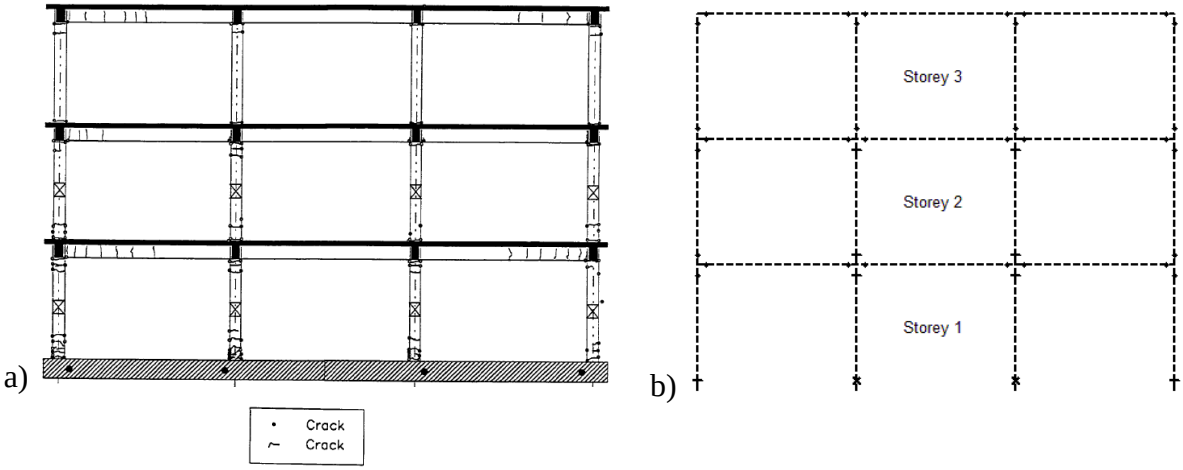

Figure 8. Damage state – Taft 0.30g: a) Experiment (Bracci, 1992); b) Analysis.

5 Damage and correlation analyses

Time history analyses of the frame subjected to 204 selected near-fault pulse-type records are performed. The damage sustained by the frame under these records is then determined using Park and Ang (1985) damage index and the commonly used inter-storey drift. The results are used for correlation analyses.

Correlation coefficient (Spiegel, 1990) is employed to analyse the inter-relation between the seismic parameters and the structural damage in terms of damage index and maximum inter-storey drift. It is worth noting that the Pearson's correlation is used for two random variables $X(X_1, X_2, \ldots, X_n)$ and $Y(Y_1, Y_2, \ldots, Y_n)$; on the contrary, the Spearman's rank correlation is used for the case of both X and Y in monotonic ranking scheme (Gibbons and Chakraborti, 2003; Spiegel, 1990). The Pearson's correlation is the case of the paper; thus, it is used. The Pearson's correlation coefficient (Gibbons and Chakraborti, 2003; Spiegel, 1990) between the above two variables is defined as shown in Equation 2, in which, $\overline{X}$ and $\overline{Y}$ are the mean values of X_i and Y_i.

$$\rho_{Pearson} = \frac{\sum_{i=1}^{n}\left(X_i - \overline{X}\right)\left(Y_i - \overline{Y}\right)}{\sqrt{\sum_{1}^{n}\left(X_i - \overline{X}\right)^2 \sum_{1}^{n}\left(Y_i - \overline{Y}\right)^2}} \tag{2}$$

The results of correlation analyses are shown in Figures 9 and 10. It is worth noting that the correlation coefficients of PGV/PGA and Mean Period are negative although for the sake of clarity, their absolute values are used in Figures 9 and 10.

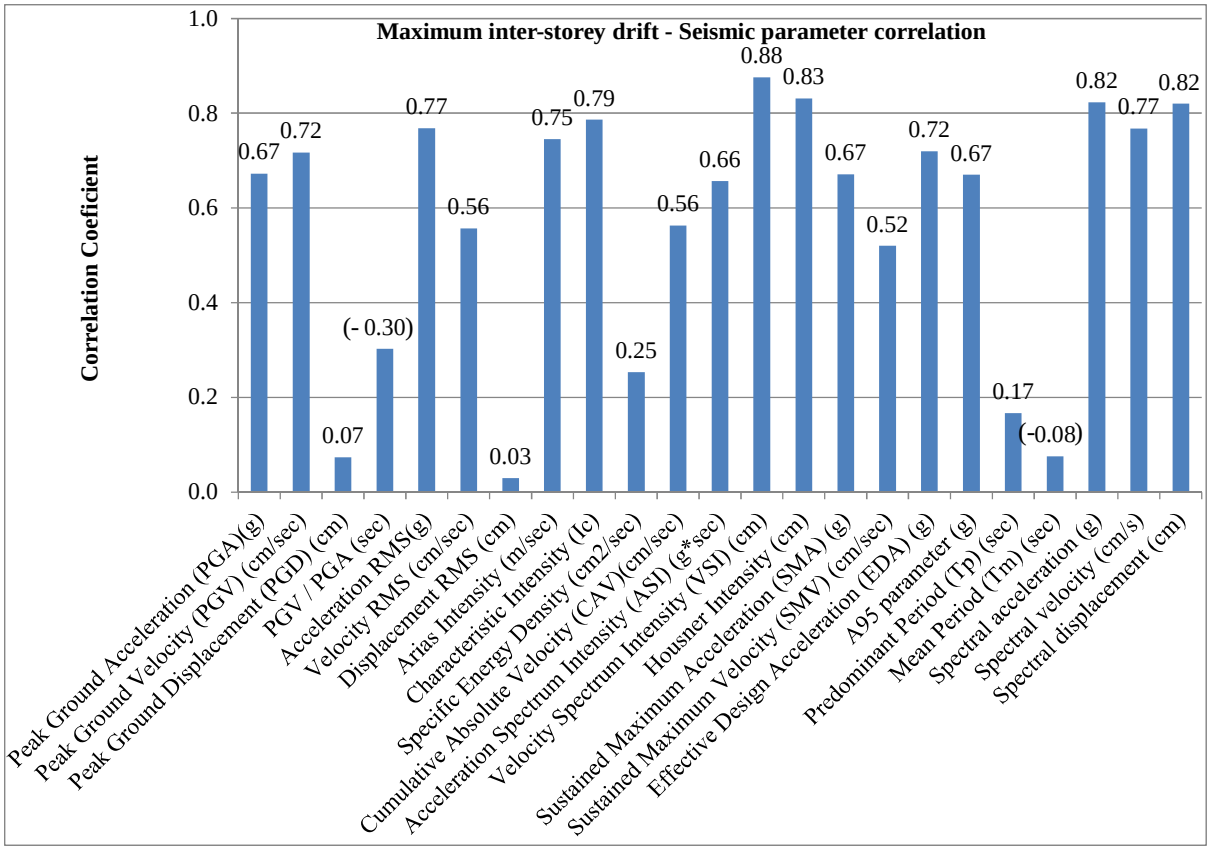

Figure 9. Correlation between maximum inter-storey drift and seismic parameters.

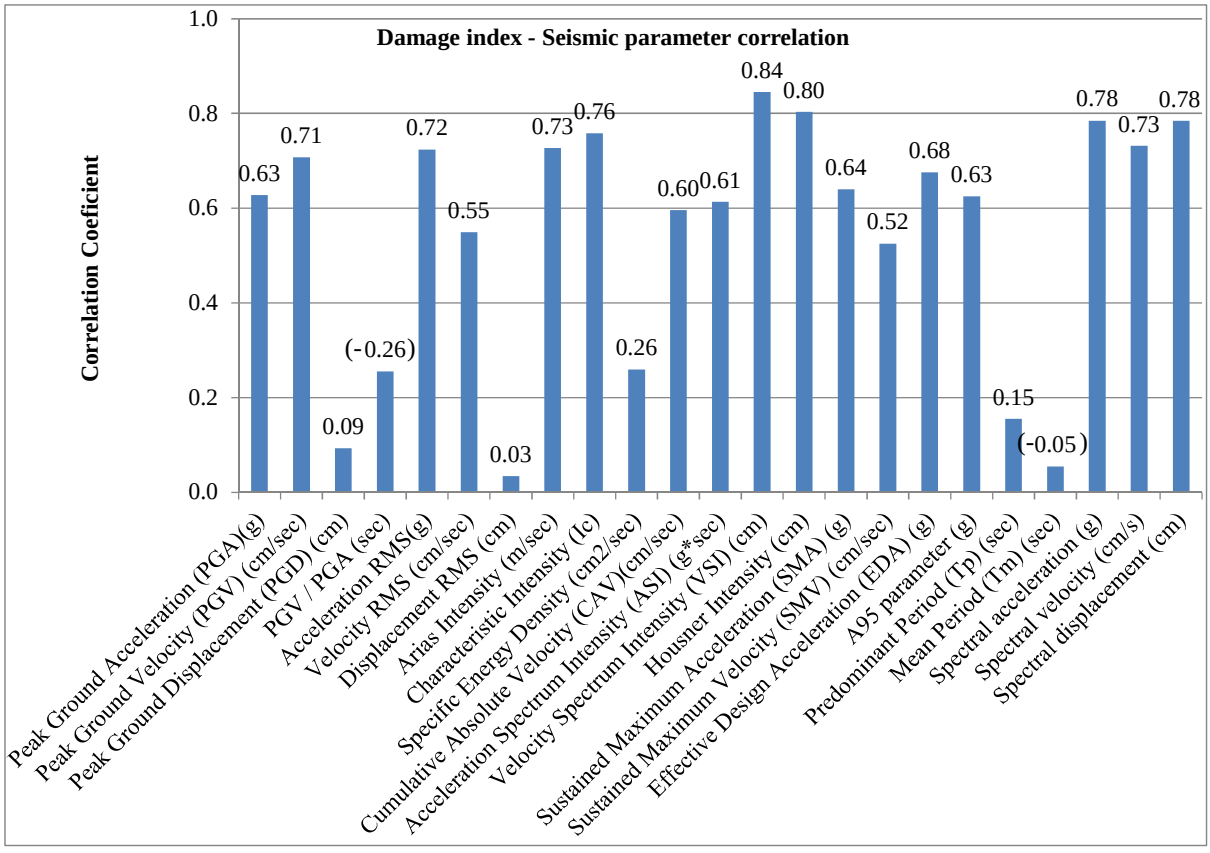

Figure 10. Correlation between Park and Ang damage indices and seismic parameters.

Amongst the 23 available seismic parameters, Velocity Spectrum Intensity demonstrates the best correlation with the damage of structures in terms of either the maximum inter-storey drift or damage index. The Housner Intensity provides the second best correlation with the damage of structures, followed by Spectral Acceleration and Spectral Displacement. Tables 8 and 9 show the order of correlation between the seismic parameters and the structural damage in terms of maximum inter-storey drift and damage index, respectively. It should be pointed out that the conventional and widely used seismic parameter of PGA does not exhibit a good correlation, which is in the order 11 or 12 as shown in Tables 8 and 9, respectively, in comparison with many others. This reaffirms the finding from previous researchers such as Elenas (1997; 2000), Elenas and Liolios (1995), Elenas *et al* (1995; 1999), and Elenas and Meskouris (2001). Displacement RMS, Peak Ground Displacement, Mean Period, Predominant Period, Specific Energy Density, PGV/PGA located in the end rows of the Tables 8 and 9 demonstrate poor correlations with the damage of the structure.

The strongest correlation of the *Velocity Spectrum Intensity* seems to be resulted from its own superiority definition, taking into account a wide range of period or frequency and the velocity. In addition, the velocity is a parameter which seems to relate to both force (acceleration) and deformation (displacement); thus, govern the damage of the structure. On the contrary, the poor correlation of parameters such as Displacement RMS, Peak Ground Displacement, Mean Period, Predominant Period can be explained by their definitions, in which only frequency or acceleration or displacement is taken into account.

Table 8. Correlation order based on maximum inter-storey drift.

Seismic parameters	**Absolute correlation coefficient**	**Order**
Velocity Spectrum Intensity (VSI) (cm)	0.8758	1
Housner Intensity (cm)	0.8307	2
Spectral acceleration (g)	0.8228	3
Spectral displacement (cm)	0.8202	4
Characteristic Intensity (Ic)	0.7861	5
Acceleration RMS(g)	0.7683	6
Spectral velocity (cm/s)	0.7677	7
Arias Intensity (m/s)	0.7456	8
Effective Design Acceleration (EDA) (g)	0.7197	9
Peak Ground Velocity (PGV) (cm/s)	0.7166	10
Peak Ground Acceleration (PGA) (g)	0.6723	11
Sustained Maximum Acceleration (SMA) (g)	0.6704	12
A95 parameter (g)	0.6700	13
Acceleration Spectrum Intensity (ASI) (g*s)	0.6565	14
Cumulative Absolute Velocity (CAV)(cm/s)	0.5628	15
Velocity RMS (cm/s)	0.5563	16
Sustained Maximum Velocity (SMV) (cm/s)	0.5200	17
PGV / PGA (s)	0.3023	18
Specific Energy Density (cm^2/s)	0.2531	19
Predominant Period (Tp) (s)	0.1667	20
Mean Period (Tm) (s)	0.0754	21
Peak Ground Displacement (PGD) (cm)	0.0732	22
Displacement RMS (cm)	0.0296	23

Table 9. Correlation order based on Park and Ang damage index.

Seismic parameters	**Absolute correlation coefficient**	**Order**
Velocity Spectrum Intensity (VSI) (cm)	0.8449	1
Housner Intensity (cm)	0.8031	2
Spectral acceleration (g)	0.7845	3
Spectral displacement (cm)	0.7840	4
Characteristic Intensity (Ic)	0.7579	5
Spectral velocity (cm/s)	0.7313	6
Arias Intensity (m/s)	0.7271	7
Acceleration RMS(g)	0.7239	8
Peak Ground Velocity (PGV) (cm/s)	0.7074	9
Effective Design Acceleration (EDA) (g)	0.6756	10
Sustained Maximum Acceleration (SMA) (g)	0.6401	11
Peak Ground Acceleration (PGA) (g)	0.6280	12
A95 parameter (g)	0.6251	13
Acceleration Spectrum Intensity (ASI) (g*s)	0.6132	14
Cumulative Absolute Velocity (CAV)(cm/s)	0.5958	15
Velocity RMS (cm/s)	0.5489	16
Sustained Maximum Velocity (SMV) (cm/s)	0.5249	17
Specific Energy Density (cm^2/s)	0.2592	18
PGV / PGA (s)	0.2557	19
Predominant Period (Tp) (s)	0.1549	20
Peak Ground Displacement (PGD) (cm)	0.0934	21
Mean Period (Tm) (s)	0.0545	22
Displacement RMS (cm)	0.0339	23

6 Conclusions

In this paper, 204 near-fault pulse-type records are selected from the Pacific Earthquake Engineering Research Center database software (PEER, 2011). Their seismic parameters are provided using the software SeismoSignal ("SeismoSignal," 2010). Time history analyses of the reinforced concrete frame representing for low-rise buildings are performed and then validated by the experimental results. Damage indices and maximum inter-storey drifts representing the damage of the frame subjected to 204 near-fault pulse-type motions are obtained from Time history analyses. Finally, the correlation coefficient is employed to

provide the degrees of inter-dependency between the damage of structure and seismic parameters. The results show that Displacement RMS, Peak Ground Displacement, Mean Period, Predominant Period, Specific Energy Density and PGV/PGA demonstrate poor correlation with the damage of structures. The conventional and widely used parameter of PGA does not exhibit a good correlation which reaffirms the conclusion from previous researchers. Velocity Spectrum Intensity provides the best correlation with the damage of structures in terms of either maximum inter-storey drift or damage index. It is followed by Housner Intensity, Spectral Acceleration and Spectral Displacement. These four are recommended as reliable parameters of near-fault pulse-type motions related to seismic damage potential of low-rise reinforced concrete structures.

7 References

ACI, (2008), Building Code Requirements for Structural Concrete (ACI 318M-08) and Commentary.

Alvanitopoulos, P.F., Andreadis, I., and Elenas, A., (2010), "Interdependence between damage indices and ground motion parameters based on Hilbert–Huang transform". *Measurement Science and Technology*, **21**. doi: 10.1088/0957-0233/21/2/025101

Arias, A., (1970), "A measure of earthquake intensity". *Cambridge,MA: MIT Press*, 438–483.

Baker, J.W., (2007), "Quantitative classification of near-fault ground motions using wavelet analysis". *Bulletin of the Seismological Society of America*, **97**(5), 1486–1501.

Banon, H., Biggs, J.M., and Irvine, H.M., (1981), "Seismic damage in reinforced concrete members". *Journal of Structural Engineering*, **107**(9), 1713–1729.

Banon, H., and Veneziano, D., (1982), "Seismic safety of reinforced members and structures". *Earthquake Engineering & Structural Dynamics*, **10**(2), 179-193.

Bassam, A., Iranmanesh, A., and Ansari, F., (2011), "A simple quantitative approach for post earthquake damage assessment of flexure dominant reinforced concrete bridges". *Engineering Structures*, **33**, 3218–3225.

Benjamin, J.R., and Associates, (1988), A criterion for determining exceedence of the operating basis earthquake *EPRI Report NP-5930*. Palo Alto, California: Electric Power Research Institute.

Bertero, V.V., Mahin, S.A., and Herrera, R.A., (1978), "Aseismic design implications of near-fault San Fernando earthquake records". *Earthquake Engineering & Structural Dynamics*, **6**(1), 31–42.

Bozorgnia, Y., and Bertero, V.V., (2001), "Evaluation of damage potential of recorded earthquake ground motion". *Seismological Research Letters*, **72**(2), 233.

Bracci, J.M., (1992), "Experimental and analytical study of seismic damage and retrofit of lightly reinforced concrete structures in low seismicity zones," State University of New York at Buffalo.

Bracci, J.M., Reinhorn, A.M., and Mander, J.B., (1995), "Seismic retrofit of reinforced concrete buildings designed for gravity loads: performance of structural system". *ACI Structural Journal*, **92**(5).

Cao, V.V., Ronagh, H., Ashraf, M., et al., (2014), "A new damage index for reinforced concrete structures". *Accepted for publication on Earthquakes and Structures*.

Choi, H., Saiidi, M.S., Somerville, P., et al., (2010), "Experimental study of reinforced concrete bridge columns subjected to near-fault ground motions". *ACI Structural Journal*, **107**(1).

Colombo, A., and Negro, P., (2005), "A damage index of generalised applicability". *Engineering Structures*, **27**(8), 1164–1174.

Computers and Structures Inc, (2009), "SAP2000 Version 14.1.0".

DiPasquale, E., Ju, J.-W., Askar, A., et al., (1990), "Relation between global damage indices and local stiffness degradation". *Journal of Structural Engineering*, **116**(5), 1440-1456.

Dobry, R., Idriss, I.M., and Ng, E., (1978), "Duration characteristics of horizontal components of strong-motion earthquake records". *Bulletin of the Seismological Society of America*, **68**(5), 1487-1520.

Eleftheriadou, A.K., and Karabinis, A.I., (2012), "Seismic vulnerability assessment of buildings based on damage data after a near field earthquake (7 September 1999 Athens - Greece)". *Earthquakes and Structures*, **3**(2), 117-140.

Elenas, A., (1997), "Interdependency between seismic acceleration parameters and the behaviour of structures". *Soil Dynamics and Earthquake Engineering*, **16**(5), 317-322.

Elenas, A., (2000), "Correlation between seismic acceleration parameters and overall structural damage indices of buildings". *Soil Dynamics and Earthquake Engineering*, **20**, 93-100.

Elenas, A., and Liolios, A., (1995), "Earthquake induced nonlinear behavior of reinforced concrete frame structures in relation with characteristic acceleration parameters". *Proceedings of the 5th International Conference on Seismic Zonation, Nice 1995*, 1013–1020.

Elenas, A., Liolios, A., and Vasiliadis, L., (1995), "Earthquake induced nonlinear behavior of structures in relation with characteristic acceleration parameters". *Proceedings of the 10th European Conference on Earthquake Engineering, Vienna 1994*, 1011-1016.

Elenas, A., Liolios, A., and Vasiliadis, L., (1999), "Correlation factors between seismic acceleration parameters and damage indicators of reinforced concrete structures". *Structural dynamics – EURODYN '99,* **2**.

Elenas, A., and Meskouris, K., (2001), "Correlation study between seismic acceleration parameters and damage indices of structures". *Engineering Structures,* **23**, 698–704.

Elnashai, A., and Sarno, L.D. (2008). *Fundamentals of Earthquake Engineering*: John Wiley & Sons, Ltd.

EPRI, (1988), A criterion for determining exceedance of the operating basis earthquake *Report No. EPRI NP-5930*. Palo Alto, California Electrical Power Research Institute.

Fajfar, P., (1992), "Equivalent ductility factors, taking into account low-cycle fatigue". *Earthquake Engineering & Structural Dynamics*, **21**, 837-848.

Fardis, M.N., Economu, S.N., Antoniou, A.N., et al., (1993), Damage measures and failure criteria - Part I, Contribution of University of Patras *Final Report of Cooperative research on the seismic response of reinforced concrete structures - 2nd Phase*.

Galal, K., and Ghobarah, A., (2006), "Effect of near-fault earthquakes on North American nuclear design spectra". *Nuclear Engineering and Design,* **236**, 1928–1936.

Galal, K., and Naimi, M., (2008), "Effect of soil conditions on the response of reinforced concrete tall structures to near fault earthquakes". *The Structural Design of Tall and Special Buildings,* **17**, 541–562.

Ghobarah, A., Abou-Elfath, H., and Biddah, A., (1999), "Response-based damage assessment of structures". *Earthquake Engineering & Structural Dynamics,* **28**, 79-104.

Ghobarah, A., and Aly, N.M., (1998), "Seismic reliability assessment of existing reinforced concrete buildings". *Journal of Earthquake Engineering*, **2**(4), 569-592.

Ghosh, S., Datta, D., and Katakdhond, A.A., (2011), "Estimation of the Park–Ang damage index for planar multi-storey frames using equivalent single-degree systems". *Engineering Structures*, **33**, 2509–2524.

Gibbons, J.D., and Chakraborti, S. (2003). *Nonparametric Statistical Inference*: Marcel Dekker, Inc.

Hatzigeorgiou, G.D., (2010), "Behavior factors for nonlinear structures subjected to multiple near-fault earthquakes". *Computers and Structures,* **88**, 309–321.

Housner, G., (1952), "Spectrum intensities of strong motion earthquakes". *Proceeding of the Symposium on earthquake and blast effects on structures in Los Angeles, California*, 20-36.

Kalkan, E., and Kunnath, S.K., (2006), "Effects of fling step and forward directivity on seismic response of buildings". *Earthquake spectra,* **22**(2), 367-390.

Kim, T.-H., Lee, K.-M., Chung, Y.-S., et al., (2005), "Seismic damage assessment of reinforced concrete bridge columns". *Engineering Structures,* **27**, 576–592.

Kramer, S.L. (Ed.), (1996), *Geotechnical Earthquake Engineering*. New Jersy: Prentice Hall.

Krishnan, S., (2007), "Case studies of damage to 19-storey irregular steel moment-frame buildings under near-source ground motion". *Earthquake Engineering & Structural Dynamics,* **36**, 861–885.

Kunnath, S.K., Reinhorn, A.M., and Lobo, R.F., (1992), "IDARC Version 3.0: A Program for the Inelastic Damage Analysis of Reinforced Concrete Structures". *Report No. NCEER-92-0022*, National Center for Earthquake Engineering Research, State University of New York at Buffalo.

Lu, L.-Y., and Lin, G.-L., (2009), "Improvement of near-fault seismic isolation using a resettable variable stiffness damper". *Engineering Structures,* **31**, 2097-2114.

Mavroeidis, G., and Papageorgiou, A., (2003), "A mathematical representation of near- fault ground motions". *Bulletin of the Seismological Society of America,* **93**(3), 1099–1131.

Mergos, P.E., and Kappos, A.J., (2009), "Seismic damage analysis including inelastic shear–flexure interaction". *Bulletin of Earthquake Engineering,* **8**, 27-46.

Mollaioli, F., Bruno, S., Decanini, L.D., et al., (2006), "Characterization of the dynamic response of structures to damaging pulse-type near-fault ground motions". *Meccanica,* **41**, 23–46.

Moustafa, A., and Takewaki, I., (2012), "Characterization of earthquake ground motion of multiple sequences". *Earthquakes and Structures,* **3**(5), 629-647.

Nanos, N., Elenas, A., and Ponterosso, P., (2008), "Correlation of different strong motion duration parameters and damage indicators of reinforced concrete structures". *The 14th World Conference on Earthquake Engineering*.

Nuttli, O.W., (1979), The relation of sustained maximum ground acceleration and velocity to earthquake intensity and magnitude *Miscellaneous paper S-73-1, Report 16* (pp. 74): U.S. Army Corps of Engineers Waterways Experiment Station,Vicksburg, Mississippi.

Ozmen, H.B., Inel, M., and Cayci, B.T., (2013), "Engineering implications of the RC building damages after 2011 Van Earthquakes". *Earthquakes and Structures*, **5**(3), 297-319.

Park, S.W., Ghasemi, H., Shen, J., et al., (2004), "Simulation of the seismic performance of the Bolu Viaduct subjected to near-fault ground motions". *Earthquake Engineering & Structural Dynamics*, **33**, 1249–1270.

Park, Y.-J., and Ang, A.H.-S., (1985), "Mechanistic seismic damage model for reinforced concrete". *Journal of Structural Engineering*, **111**(4), 722-739.

PEER. (2011). PEER ground motion database. http://peer.berkeley.edu/peer_ground_motion_database.

Powell, G.H., and Allahabadi, R., (1988), "Seismic damage prediction by deterministic methods: Concepts and procedures". *Earthquake Engineering & Structural Dynamics*, **16**, 719-734.

Rathje, E.M., Abrahamson, N.A., and Bray, J.D., (1998), "Simplified frequency content estimates of earthquake ground motions". *Journal of Geotechnical and Geoenvironmental Engineering*, **124**(2), 150–159. doi: 10.1061/(ASCE)1090-0241(1998)124:2(150)

Rodriguez, M.E., and Padilla, D., (2009), "A damage index for the seismic analysis of reinforced concrete members". *Journal of Earthquake Engineering*, **13**(3), 364-383.

Roufaiel, M.S.L., and Meyer, C., (1981), "Analysis of damaged concrete frame buildings". *Technical Report No. NSF-CEE-81-21359-1*, Columbia University, New York.

Roufaiel, M.S.L., and Meyer, C., (1987), "Analytical modeling of hysteretic behavior of R/C frames". *Journal of Structural Engineering, ASCE*, **113**(3), 429–444.

Sarma, S.K., and Yang, K.S., (1987), "An evaluation of strong motion records and a new parameter A95". *Earthquake Engineering & Structural Dynamics*, **15**(1), 119-132.

. SeismoSignal (Version 4.1.2). (2010). Pavia, Italy: Seismosoft Ltd. Retrieved from http://www.seismosoft.com/en/HomePage.aspx

Sheikh, S.A., and Khoury, S.S., (1993), "Confined concrete columns with stubs". *ACI Structural Journal*, **90**(4), 414-431.

Spiegel, M.R. (Ed.), (1990), *Theory and problems of statistics*. London: McGraw-Hill.

Tabeshpour, M.R., Bakhshi, A., and Golafshani, A.A., (2004), "Vulnerability and damage analyses of existing buildings". *13th World Conference on Earthquake Engineering*, **Paper No. 1261**.

Takeda, T., Sozen, M.A., and Nielsen, N.N., (1970), "Reinforced concrete response to simulated earthquakes". *Journal of the Structural Division,* **96**, 2557-2573.

Thun, J.L.V., Roehm, L.H., Scott, G.A., et al., (1988), "Earthquake ground motions for design and analysis of dams". *Geotechnical special publication: Earthquake Engineering and Soil Dynamics II—Recent Advances in Ground-Motion Evaluation,* **20**, 463-481.

Yon, B., Sayin, E., and Koksal, T.S., (2013), "Seismic response of buildings during the May 19, 2011 Simav, Turkey earthquake". *Earthquakes and Structures*, **5**(3), 343-357.

Yüksel, E., and Sürmeli, M., (2010), "Failure analysis of one-story precast structures for near-fault and far-fault strong ground motions". *Bulletin of Earthquake Engineering,* **8**, 937–953.